Int. J. of Thermal & Environmental Engineering
Volume 6, No. 1 (2013) 21-26

Energy Optimization of Heat Engine with Infinite Heat Capacity Reservoirs

Christer Nylund [a], M. El Haj Assad [b,] *
[a] *Arcada University of Applied Sciences, Jan-Magnus Janssonin aukio 1*
[b] *Aalto University, School of Science and Technology, Department of Energy Technology, 00076 Aalto, Finland*

Abstract
The optimal energy output of a heat engine based on the Carnot process is studied. The internal irreversibility of the engine is considered by taking into account the entropy generation in the adiabatic processes. The engine is connected to high and low temperature thermal energy reservoirs with infinite heat capacity. The process temperatures and the energy conductivity of heat exchangers that maximizes the energy output have been obtained. The effect of the internal irreversibility on the optimal performance of the engine is shown. Two numerical examples are given.

Keywords: *Heat engine, Irreversibility, Work.*

1. Introduction

There is a huge need for designing a heat engine that runs at a finite speed in order to produce power. In reality, the reversible performance limits of a heat engine to produce power is not reached and these reversible performance limits are set to be the upper performance limits of a real heat engine. The research work for searching the performance limits of a heat engine was presented by Curzon and Ahlborn [1] by introducing finite-time thermodynamics. Their heat engine considered the external irreversibilities due to the finite temperature difference between the heat engine and its surrounding but did not consider the internal irreversibilities within the heat engine; such heat engine is called an endoreversible heat engine. Finite-time thermodynamics has been applied as an effective tool to optimize the performance of an irreversible magneto hydrodynamic power plant using magneto hydrodynamic generator (MHD) running at constant velocity and constant Mach number [2-7].

The general performance characteristics of an irreversible refrigerator using nonlinear heat transfer law has been investigated [8] by considering the internal irreversibility as well as the external irreversibility. Finite-time thermodynamics has been used to analyze the performance of an irreversible heat engine with temperature dependent heat capacities of a working fluid [9], to obtain optimal expansion of a working fluid with convective radiative heat transfer [10] and to investigate the effects of variable specific heat ratio of the working fluid on the performance of an irreversible Diesel cycle [11]. Recently, finite-time thermodynamics has been applied as an effective and efficient tool to optimize the performance of heat engines, heat pumps and refrigerators [12-23]. In general, entropy generation analysis is an important and effective tool to design a heat engine like combined diesel-engine gas-turbine system [24] and a heat pump like absorption cycles [25].

The main objective of this work is to optimize the performance of an irreversible heat engine (real heat engine) and to study the effect of the internal irreversibility on engine performance.

2. Cycle Model

The heat engine is working between an infinite heat source at temperature T_H and an infinite heat sink at temperature T_C. The *T-S* diagram of an irreversible heat engine is shown in Figure 1. Heat is added to the engine from the heat source and rejected from the engine to the heat sink. There are four processes in the engine cycle, each changing the state of the working fluid. The heat engine is operating with two isothermal and two adiabatic processes. The four processes are summarized as:
State 1-state 2: Adiabatic compression, temperature change from T_{14} to T_{23} and entropy change from S_1 to S_2 marked as ΔS_{12}.

* Corresponding author. Tel.: +358504315582
Fax: +35894702341; E-mail: mamdouh.assad@aalto.fi

DOI: 10.5383/ijtee.05.01.004

State 2-state 3: Isothermal expansion, heat addition of Q_H at constant temperature T_{23} and entropy change from S_2 to S_3 marked as ΔS_{23}.
State 3-state 4: Adiabatic expansion, temperature change from T_{23} to T_{14} and entropy change from S_3 to S_4 marked as ΔS_{34}.
State 4-state 1: Isothermal compression, heat rejection of Q_C at constant temperature T_{14} and entropy change from S_4 to S_1 marked as ΔS_{14}.

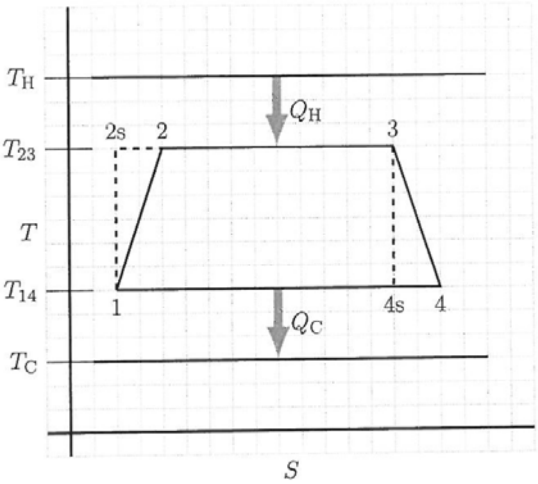

Fig. 1.T-S diagram of an internally irreversible heat engine

The heat addition and heat rejection of the heat engine can be written as, respectively

$$Q_H = G_H(T_H - T_{23}) = \Delta S_{23} T_{23} \tag{1}$$

$$Q_C = G_C(T_{14} - T_C) = \Delta S_{14} T_{14} \tag{2}$$

where G_H and G_C are the energy transfer ability (the overall energy transfer coefficient × transfer area) of the corresponding heat exchanger.

An internal irreversibility parameter, σ, and a variable, τ, are defined to describe the processes of the heat engine. The parameter σ ($0 \le \sigma \le 1$) will take into account the internal irreversibility of the adiabatic processes and the variable τ ($0 < \tau < 1$) is the ratio of the minimum and maximum temperatures of the real cycle (note that the minimum and maximum temperatures of the reversible cycle are T_H and T_C). The internal irreversibility parameter and the temperature ratio can be written as

$$\sigma = \frac{\text{entropy change, isothermal expansion}}{\text{entropy change, isothermal compression}} = \frac{\Delta S_{23}}{\Delta S_{14}} \tag{3}$$

$$\tau = \frac{\text{minimum temperature, cycle}}{\text{maximum temperature, cycle}} = \frac{T_{14}}{T_{23}} \tag{4}$$

The variable ς ($0 < \varsigma < 1$) which takes into account the heat energy transfer ability of the heat source exchanger, is defined as

$$\varsigma = \frac{G_H}{G_H + G_C} = \frac{G_H}{G_t} \tag{5}$$

where $G_t = G_H + G_C$ is the total energy transfer of the heat exchangers.

The work output of the heat engine can be expressed as

$$W = Q_H - Q_C = Q_H\left(1 - \frac{T_{14}\Delta S_{14}}{T_{23}\Delta S_{23}}\right) = Q_H\left(1 - \frac{\tau}{\sigma}\right) \tag{6}$$

Using equations (1-5), equation (6) can be written in the following form

$$\Omega(\varsigma, \tau) = \frac{W}{G_t T_H} = \frac{\varsigma}{\tau} \cdot \frac{\tau - \tau_o}{\left(1 + \frac{1}{\sigma} \cdot \frac{\varsigma}{1 - \varsigma}\right)}\left(1 - \frac{\tau}{\sigma}\right) \tag{7}$$

where Ω is the dimensionless work output of the heat engine which is a function of two variables, ς and τ, and two constants, σ and $\tau_o = \frac{T_C}{T_H}$.

3. Optimum work output

The work output of the heat engine, Ω, is maximized with respect to ς and τ by solving the following equations simultaneously

$$\left(\frac{\partial \Omega}{\partial \varsigma}\right)_\tau = 0 \tag{8}$$

$$\left(\frac{\partial \Omega}{\partial \tau}\right)_\varsigma = 0 \tag{9}$$

Solving the derivatives given in equations (8) and (9) and taking into account the constrains of the parameters ς, τ and σ [($0 < \varsigma < 1$), ($0 < \tau < 1$) and ($0 < \sigma \le 1$)] give the following optimum parameters

$$\varsigma_{\text{opt}} = \frac{\sqrt{\sigma}}{1 + \sqrt{\sigma}} \tag{10}$$

$$\tau_{\text{opt}} = \sqrt{\sigma \frac{T_C}{T_H}} \tag{11}$$

The efficiency of the heat engine at optimal energy output is obtained as

$$\eta_{\text{opt}} = 1 - \sqrt{\frac{T_C}{\sigma T_H}} \tag{12}$$

Using equations (6), (10) and (11), the optimal dimensionless energy output is obtained as

$$\Omega_{\text{opt}} = \sigma \left(\frac{1 - \sqrt{\frac{1}{\sigma}\frac{T_C}{T_H}}}{1 + \sqrt{\sigma}} \right)^2 \tag{13}$$

The optimal process temperatures of the heat addition and heat rejection are expressed as, respectively

$$T_{14,\text{ opt}} = \frac{T_C + \sqrt{T_C T_H}}{1 + \frac{1}{\sqrt{\sigma}}} \tag{14}$$

$$T_{23,\text{ opt}} = \frac{T_H + \sqrt{T_C T_H}}{1 + \sqrt{\sigma}} \tag{15}$$

For an internally reversible heat engine (isentropic compression and expansion processes), for which the internal irreversibility parameter is equal to 1, equations (10-15) can be written as, respectively

$$\varsigma_{\text{opt, s}} = 0.5 \tag{16}$$

$$\tau_{\text{opt, s}} = \sqrt{\frac{T_C}{T_H}} \tag{17}$$

$$\eta_{\text{opt, s}} = 1 - \tau_{\text{opt, s}} \tag{18}$$

$$\Omega_{\text{opt, s}} = 0.25 \left(\eta_{\text{opt, s}}\right)^2 \tag{19}$$

$$T_{14\text{s, opt}} = 0.5\left(\mathrm{T_C} + \sqrt{\mathrm{T_C T}_H}\right) \tag{20}$$

$$T_{23\text{s, opt}} = 0.5\left(\mathrm{T_H} + \sqrt{\mathrm{T_C T}_H}\right) \tag{21}$$

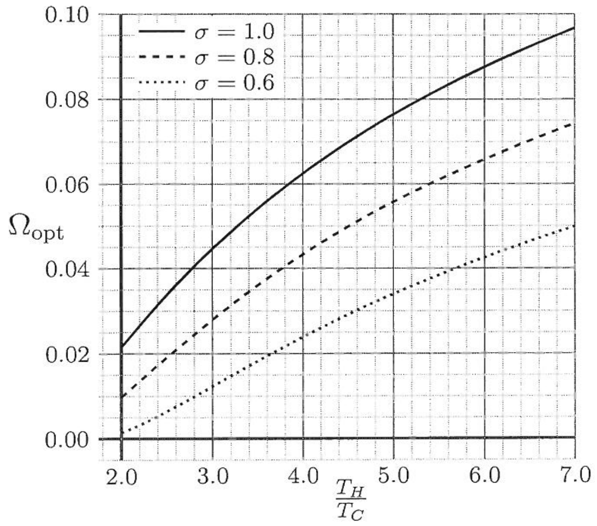

Fig. 2. Optimal dimensionless work output

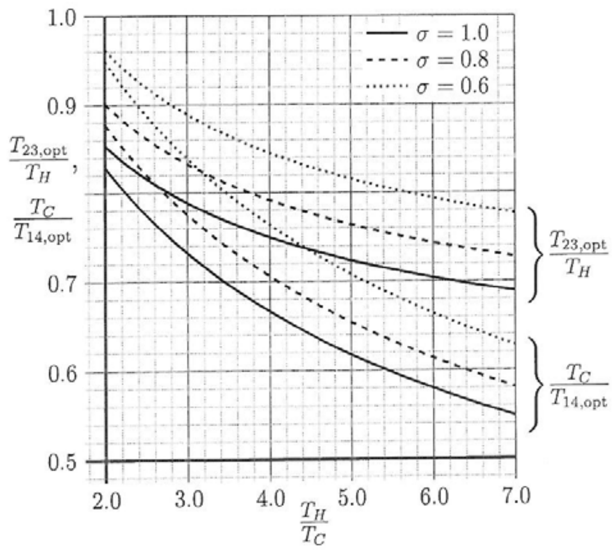

Fig. 3. Optimal dimensionless process temperatures

4. Results

The optimum dimensionless work output obtained in equation (13) is function of the irreversibility parameter (σ) and the temperature ratio $\frac{T_C}{T_H}$. The effect of the temperature ratio $\frac{T_H}{T_C}$ on the work output is demonstrated in Figure 2 for different values of internal irreversibility parameter. Figure 2 shows that the work output increases as the temperature ratio $\frac{T_H}{T_C}$ increases for all values of the internal irreversibility parameter. The figure also shows that the heat engine produces maximum work output for reversible engine, i.e. for $\sigma = 1$ and as σ decreases the work output decreases. Using equations (14) and (15), the effect of temperature ratio $\frac{T_H}{T_C}$ on the optimum temperatures T_{23} and T_{14} can be investigated as shown in Figure 3 for different values of the internal irreversibility parameter.

4.1. Example 1

The idea with this example is to show how the optimal work output, optimal process temperatures and other optimal variables depend on the internal irreversibility in the adiabatic processes. The calculation is done for $T_H = 1200$ K, $T_C = 300$ K, $G_t = 1$ MJ/K and $\sigma = 0.6$, 0.8 and 1. The results are shown in Table 1. Table 1 shows that the optimal energy output is decreasing more rapidly than the optimal efficiency with increasing irreversibility in the adiabatic processes. As the internal irreversibility parameter approaches zero then $T_{14,\text{opt}} \to T_C$ and $T_{23,\text{opt}} \to T_H$, therefore $Q_{H,\text{opt}}(\sigma < 1) < Q_{H,\text{opt}}(\sigma = 1)$ and $Q_{C,\text{opt}}(\sigma < 1) < Q_{C,\text{opt}}(\sigma = 1)$. The real reason for that is η_{opt} decreases with decreasing ς_{opt} and Ω_{opt} is proportional to ς^2_{opt} . The total energy transfer of the heat exchangers should be divided so that $G_H = G_C$ for $\sigma = 1$, and the amount of G_C should increase with decreasing σ .

4.2. Example 2

Steam power plant operating on a modified Rankine cycle. The steam enters the turbine at 400 °C and 2 MPa and is condensed in the condenser at a pressure of 50 kPa. The isentropic efficiency of the turbine and the feed pump are 80 respective 70 %.

The thermodynamic average temperature during the heating and the cooling processes are (using $Tds = dh - vdp$, and assuming constant pressure)

$$\bar{T}_{\text{proc}} = \frac{h_{\text{exit}} - h_{\text{inlet}}}{s_{\text{exit}} - s_{\text{inlet}}} = \frac{\Delta h_{\text{proc}}}{\Delta s_{\text{proc}}}$$

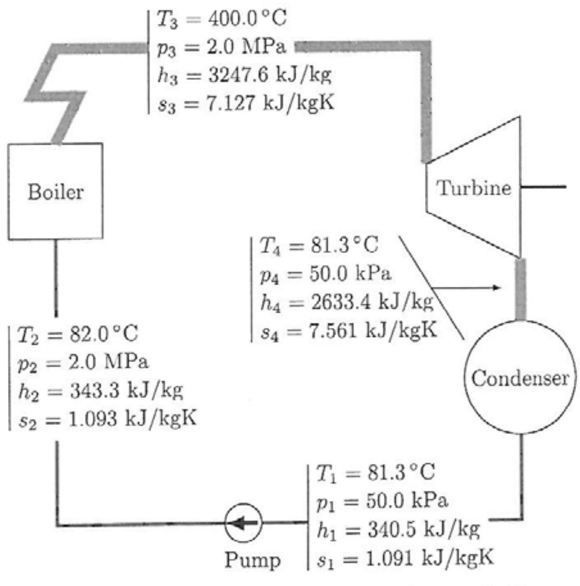

Fig. 4. Rankine cycle (example 2)

The model presented in this paper is supported by the following two numerical examples.

$$\sigma = \frac{\Delta s_{23}}{\Delta s_{14}} = \frac{7.127 - 1.093}{7.561 - 1.091} = 0.933$$

The optimal temperatures of the heat source and the heat sink can now be calculated, using equation (14) and equation (15). Dividing equation (14) by equation (15), we obtain

$$\sqrt{\frac{T_C}{T_H}} = \frac{1}{\sigma}\frac{\bar{T}_{14}}{\bar{T}_{23}} = 0.762$$

Adding equation (14) to equation (15), we get

$$\sqrt{T_H} + \sqrt{T_C} = \sqrt{\left(1 + \sqrt{\sigma}\right)\left(\frac{\bar{T}_{14}}{\sqrt{\sigma}} + \bar{T}_{23}\right)} = 40.84$$

For the heating process the thermodynamic average temperature is calculated according to the thermodynamic state values given in Figure 4, as

$$\bar{T}_{23} = \frac{\Delta h_{23}}{\Delta s_{23}} = \frac{3247.6 - 343.3}{7.127 - 1.093} = 481.3\,\text{K}$$

and for the cooling process the thermodynamic average temperature as,

$$\bar{T}_{14} = \frac{\Delta h_{14}}{\Delta s_{14}} = \frac{2633.4 - 340.5}{7.561 - 1.091} = 354.4\,\text{K}$$

The internal irreversibility parameter is calculated from equation (3) as

From the last two equations, the temperatures T_H and T_C can be solved as $T_H = 537.2$ K and $T_C = 311.9$ K.

The efficiency of the modified Rankine cycle at the maximum work output is obtained from equation (12) as

$$\eta_{opt} = 1 - \sqrt{\frac{1}{\sigma}\frac{T_C}{T_H}} = 0.211$$

For the modified Rankine cycle in Figure 4, the thermal efficiency is

$$\eta = \frac{w_T - w_P}{q_B} = \frac{(h_3 - h_4) - (h_2 - h_1)}{h_3 - h_2} = 0.211$$

which is exactly the same as the efficiency at optimal work output.

5. Conclusion

In this work the performance characteristic of an irreversible heat engine with internal and external irreversibilities was investigated. The internal irreversibility is described by a single parameter and the effect of this parameter on the engine performance was obtained. An expression for the optimum work of the heat engine is derived.

The results show that the internal irreversibility parameter has a crucial effect on the heat engine performance. The mathematical model is supported by Rankine cycle example in order to calculate the internal irreversibility parameter and the real thermal cycle efficiency which is well below Carnot efficiency. Hence, calculations of the same type as Curzon and Ahlborn [1] did, but done as energy equilibrium calculations, is an effective tool to find the performance limits of real heat engine.

Table 1. Results of example 1

σ	ς_{opt}	τ_{opt}	η_{opt}	Ω_{opt}	$G_{H,opt}$ [MJ/K]	$G_{C,opt}$ [MJ/K]	$T_{14,opt}$ [K]	$T_{23,opt}$ [K]
1.0	0.500	0.500	0.500	0.0625	0.500	0.500	450	900
0.8	0.472	0.447	0.441	0.0433	0.472	0.528	425	950
0.6	0.436	0.387	0.355	0.0239	0.436	0.564	393	1014

References

[1] Curzon F. L., Ahlborn B. Efficiency of a Carnot engine at maximum power output. *American J. Physics*, 1975, 43(1): 22-24.

[2] El Haj Assad M. Characteristics of thermal cycles and energy conversion systems. *Acta Polytechnica Scandinavica*, Mechanical Engineering Series, 1998(130): 1-35.

[3] El Haj Assad M., Wu C. Finite-time thermodynamics of a MHD power plant. Recent Advances in Finite-Time Thermodynamics, Editors: Chih Wu, Lingen Chen and Jincan Chen, New York: Nova Science Publishers, 1999.

[4] El Haj Assad M. Thermodynamic analysis of an irreversible MHD power plant. *Int. J. Energy Research*, 2000, 24(10): 865-875.

[5] El Haj Assad M., Wu C. Performance of a regenerative MHD power plant. *Int. J. Power and Energy Systems*, 2004, 24(2): 98-103.

[6] El Haj Assad M. Optimum performance of a regenerative MHD power plant. *Int. J. Exergy*, 2007, 24(1): 87-97.

[7] El Haj Assad M., Wu C. Thermodynamic performance of an irreversible MHD power cycle running at constant Mach number. *Int. J. Ambient Energy*, 2008, 29(1): 27-34.

[8] El Haj Assad M. Performance characteristics of an irreversible refrigerator. *Int. J. Energy, Environment and Economics*. 2000, 10 (2).

[9] Liu J., Chen J. Optimum performance analysis of a class of typical irreversible heat engines with temperature-dependent heat capacities of the working substance. *Int. J. Ambient Energy*, 2010, 31(2): 59-70.

[10] Chen L., Song H., Sun F., Wu C. Optimal expansion of a heated working fluid with convective radiative heat transfer law. *Int. J. Ambient Energy*, 2010, 31(2): 81-90.

[11] Ebrahimi R., Chen L. Effects of variable specific heat ratio of working fluid on the performance of an irreversible Diesel cycle. Int. J. Ambient Energy, 2010, 31(2): 101-108.

[12] Feng H., Chen L., Sun F. Finite time exergoeconomic performance optimization for an irreversible universal steady flow variable-temperature heat reservoir heat pump cycle model. *Int. J. Energy and Environment*, 2010, 1(6):969-986.

[13] Chen L., Yang B., Sun F. Exergoeconomic performance optimization of an endoreversible intercooled regenerated Brayton cogeneration plant. Part 1: Thermodynamic model and parameter analyses. *Int. J. Energy and Environment*, 2011, 2(2):199-210.

[14] Yang B., Chen L., Sun F. Exergoeconomic performance optimization of an endoreversible intercooled regenerated Brayton cogeneration plant. Part 2: Heat conductance allocation and pressure ratio optimization. *Int. J. Energy and Environment*, 2011, 2(2):211-218.

[15] Ding Z., Chen L., Sun F. Performance characteristic of energy selective electron (ESE) heat engine with filter heat conduction. *Int. J. Energy and Environment*, 2011, 2(4):627-640.

[16] Liu X., Chen L., Wu F., Sun F. Cooling load and COP optimization of an irreversible Carnot refrigerator with spin-1/2 systems. *Int. J. Energy and Environment*, 2011, 2(5):797-812.

[17] Chen L., Kan X., Wu F., Sun F. Finite time exergoeconomic performance of a thermoacoustic cooler with a complex heat transfer exponent. *Int. J. Energy and Environment*, 2012, 3(1):19-32.

[18] Liu C., Chen L., Sun F. Endoreversible Meletis-Georgiou cycle. *Int. J. Energy and Environment*, 2012, 3(2):305-322.

[19] Xia S., Chen L., Sun F. Hamilton-Jacobi-Bellman equations and dynamic programming for power-optimization of radiative law multistage heat engine system. *Int. J. Energy and Environment*, 2012, 3(3):359-382.

[20] Zhang Z., Chen L., Sun F. Exergy analysis for combined regenerative Brayton and inverse Brayton cycles. *Int. J. Energy and Environment*, 2012, 3(5):715-730.

[21] Yang B., Chen L., Sun F. Exergoeconomic performance optimization of an endoreversible intercooled regenerative Brayton combined heat and power plant coupled to variable-temperature heat reservoirs. *Int. J. Energy and Environment*, 2012, 3(4):505-520.

[22] Chen L., Kan X., Sun F., Wu F. Exergoeconomic performance optimization for a steady-flow endoreversible refrigeration model including six typical cycles. *Int. J. Energy and Environment*, 2013, 4(1):93-102.

[23] El Haj Assad M. Cooling load optimization of an irreversible refrigerator with combined heat transfer. *Int. J. Energy and Environment*, 2013, 4(3):377-386.

[24] El-Awad M. Energy and exergy analysis of a combined diesel-engine gas-turbine system for distributed power generation. *Int. J. of Thermal & Environmental Engineering*, 2013, 5(1):31-39.

[25] Ayou D.S., Bruno J.C., Coronas A. New power and cooling absorption cycles. *Int. J. of Thermal & Environmental Engineering*, 2013, 5(2):135-143.